

Hydrodynamics of domain relaxation in a polymer monolayer

E. K. Mann,* S. Hénon, D. Langevin, and J. Meunier

Laboratoire de Physique Statistique de l'Ecole Normale Supérieure, 24, rue Lhomond, 75231 Paris Cedex 05, France

L. Léger

Physique de la Matière Condensée, Collège de France, Place Berthelot, 75231 Paris Cedex 05, France

(Received 27 December 1994)

The line tension between two phases within a monolayer can be determined from the characteristic relaxation time of deformed domains, if the hydrodynamics of that relaxation, in particular the relative roles of surface and bulk viscosity, can be established. This is accomplished here for a polymer monolayer by varying the viscosity of the bulk substrate. A Poly(dimethyl)siloxane monolayer segregates into dense and dilute polymer domains on aqueous glycerol and glucose solutions (of viscosity $1.2 < \eta/\eta_{\text{water}} < 75$) as well as on pure water. The surface pressures of these polymer films are, for moderate surface pressures and within experimental precision, independent of the glycerol and glucose content of the substrate solutions. Isolated polymer domains relax toward the circular form, linearly for the early "bola" form and exponentially for moderate deformations. Relaxation times T_c are measured for domains of size $10 \mu\text{m} < R < 80 \mu\text{m}$ and $0.2 \text{ sec} < T_c < 60 \text{ sec}$. Relaxation of monolayer domains in the two limits, in which surface or bulk viscosity dominates, is discussed. All data are consistent with dissipation dominated by viscosity in the substrate. The deduced line tension is $\lambda = (1.1 \pm 0.3) \times 10^{-12} \text{ N}$.

PACS number(s): 68.10.-m, 68.15.+e, 47.55.Dz, 47.15.Gf

INTRODUCTION

Monomolecular films on liquid surfaces have been studied for more than 100 years and the possibility of different states or phases in these films, analogous to those in three dimensions, was introduced quite early, along with the possibility of phase coexistence [1]. However, it is only in the past 10 years that direct visualization of monomolecular films has become possible: first by way of fluorescence microscopy [2], in which fluorescent probes with different solubilities in different phases are introduced into the film, and later by microscopy at the Brewster angle [3], which uses directly the differing reflectivity, because of different optical densities, of different phases.

The monolayers studied have displayed a very wide range of domain shapes and behavior [4]. Dynamic growth factors play an important role and true equilibrium appears to be difficult to achieve in such monolayer systems. The underlying equilibrium situation is assumed to be governed by intermolecular forces as divided into two distinct contributions: short-range interactions, which can be characterized by a size- and shape-independent line tension (which nonetheless may be anisotropic if the phases are [5]), in analogy with the surface tension of a three-dimensional object, and long-range interactions, which cannot. These long-range interactions are assumed to be electrostatic in origin. Virtually any molecule forming a film on the water surface will be ei-

ther charged or polar and since it will tend to be aligned with respect to the surface, a net dipole moment perpendicular to the surface is nearly universal. The surface potential was in fact one of the earliest means of characterizing monomolecular films [1]. The electrostatic contribution may be estimated by this or a variety of other methods [6].

The first experimental estimates of the line tension in such systems are very recent [5,7,8]. Most direct methods for measuring the analogous surface tension in three-dimensional systems make use of a balance between surface tension and gravitational forces: this includes the pendant or sessile drop, the capillary rise, and the various Wilhelmy methods. There is no obvious equivalent in the two-dimensional monolayer. Of other methods commonly useful in three dimensions, thermally excited capillary waves [9] would provide one measure, but in the absence of a probe of the line equivalent to surface light scattering, one is currently limited to cases in which the excitations are large enough to see, that is on the micrometer scale, corresponding (for typical domain sizes $\sim 100 \mu\text{m}$) to line tensions $\lambda \leq 10^{-14} \text{ N}$. These are very small values: the equivalent of 10 mN/m in three dimensions would be $\lambda \sim 10^{-11} \text{ N}$ (assuming a typical nanometer thickness) on the monolayer level. Fluctuations in domain shape consistent with thermal fluctuations have been observed [10], but only under special conditions, near a critical point, for example. Forced capillary waves can provide a convenient estimation of larger surface tensions, but again these are at this time impractical in monolayer systems: one needs a sufficiently local method of excitation (and also a means of holding the average line position fixed for observation, again in the absence of the gravitational forces convenient in three dimensions). A further com-

*Present address: Institut Charles Sadron, 6 rue Boussingault, 67083 Strasbourg Cedex, France.

plication is that one expects to be in the overdamped limit: material movement in the monolayer necessarily drags along the substrate, providing sufficient resistance to reach this limit even in the absence of significant surface viscosity [11]. An understanding of the viscous properties of the system and their influence on line movement would thus be necessary to deduce the line tension from such a method.

One is thus led to find other, often more indirect, methods of measuring the line tension in these systems. Observation suggests using the relaxation of deformed domains to an equilibrium shape; a similar method has been used in three dimensions when other techniques appeared inconvenient [12]. The minimization of line energy drives this relaxation; the pressure difference across the domain boundary, given by the Laplace law as λ/R_c , where R_c is the local radius of curvature, leads to pressure gradients, and thus monolayer movement, within noncircular domains. Since again we expect to be in the overdamped regime, these would be opposed and balanced by viscous forces: the surface viscosity in the monolayer, the drag due to the viscosity of the substrate if there is material transport (i.e., if the different phases have significantly different densities), and conceivably viscous drag of the monolayer against the substrate, though this is expected to be sufficiently large to preclude such movement. The bulk viscosity is known; in principle, the surface viscosity of a monolayer can be measured (though this is delicate and may depend on the time scale).

In practice, the hydrodynamical problem is sufficiently difficult even when one of the terms dominates; this is therefore assumed. The different assumptions lead to distinctive behavior either in function of the size of the domain [8] or in mode [13], which can then be tested.

In this way, we were led to conclude tentatively that viscous drag during such relaxation in a polymer [poly(dimethyl)siloxane (PDMS)] layer was dominated by the surface viscosity [8]. Experimental limitations confined these measurements to a relatively narrow range of sizes and relaxation times (between 10 and 50 μm and between 2 and 10 sec). A larger range is desirable, along with a direct test to the hypothesis, by changing, for example, the bulk viscosity. This seemed all the more important because the relaxation times were found to be independent of polymer mass, which would imply that the surface viscosity was surprisingly independent of this parameter.

Here we extend the experiment to smaller relaxation times and vary the substrate viscosity by adding glycerol or glucose. Since the monolayer properties may change with the changing substrate, an initial test of this possibility is made through comparisons of the surface pressure isotherms on examples of these different substrates.

The polymer is PDMS, which at low concentrations on pure water forms compact domains of polymer chains stretched flat on the surface (a long-standing hypothesis [14] recently demonstrated by neutron reflectivity studies [15]) in coexistence with a very dilute polymer gas [8]. As the concentration is increased, the polymer undergoes a complicated collapse process, in which polymer layers of

different thickness are observed in coexistence with three-dimensional polymer droplets. In the previous relaxation study [8], domains were observed in both the submonolayer regime and in one of the multilayer regimes (where the "multilayers" may be that, or single layers in which the polymer takes on different, less stretched out conformations with respect to the surface). Here measurements are confined to the submonolayer regime, under better-controlled experimental conditions than were available for the preliminary work. In contrast to that study [8], we find that the dissipation is dominantly due to the substrate, consistent with the observation that relaxation times are independent of the molecular mass of the polymer.

EXPERIMENTAL METHODS

Microscopy at the Brewster angle, described in detail elsewhere [3], was recently developed to study films of amphiphilic molecules at the air-liquid interface. It takes advantage of the reflective properties of an interface when illuminated with light polarized in the plane of incidence. This reflectivity r_p^2 has a minimum for incidence at the Brewster angle and since this minimum would be null if the interface was perfectly smooth and abrupt, it is very sensitive to the interfacial properties: its roughness, thickness, and anisotropy. Coexistence of different phases of a monolayer or between multilayers of different thicknesses can thus be observed [3,8,16].

With the objective used in this work, the resolution of the microscope is $\sim 1.5 \mu\text{m}$ and the field of view (and illuminated area) $\sim 700 \mu\text{m}$. Images must be collected by bands, moving the objective between each band: the $\sim 53^\circ$ angle of reflectivity means that the distance between objective and surface is constant and the image in focus only along a line for a given position of the objective with respect to the surface. This presently limits the recording of images to 0.3 images/sec. To study faster re-

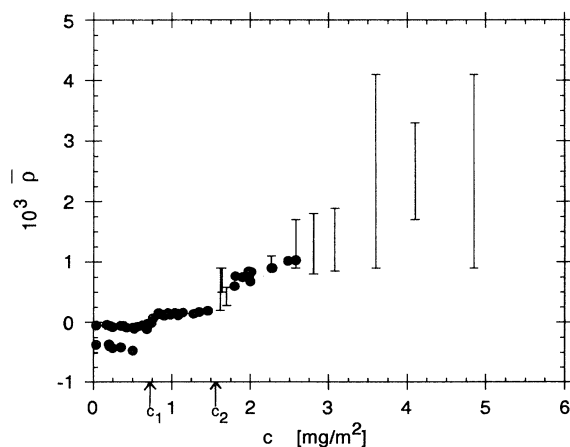


FIG. 1. Ellipticity $\bar{\rho}_B$ as a function of polymer concentration on pure water. Estimated errors are 10% on $\bar{\rho}_B$ and 5% on c , on the order of the data symbol size. Bars represent fluctuations in the ellipticity out of this range due to inhomogeneities in the surface films.

laxation, thin bands may be collected at rates up to 10 images/sec, depending on the band size. These are, however, out of focus over most of the band, leading to characteristic halos at the domain boundaries [see Fig. 4(c)]; the width of the halo depends on the position of that domain edge with respect to the focal plane.

The method is limited to films in which the optical index of refraction of the film is different from that of the substrate. The reflective intensity at the Brewster angle $I_0 r_p^2$ is proportional to the square of the ellipticity (which is equal to r_p/r_s , the ratio between the reflectivities for the two different polarizations; r_s varies little with the presence of the film). This ellipticity is shown in Fig. 1 for the system PDMS on pure water; the experiments described here are in the region well below what is labeled c_1 . The observed contrast is that between the two ellipticity levels at these concentrations [17], proportional by the Drude law [18] to the difference in refractive index between film and substrate. The substrates for the experiments reported here were a series of glycerol and glucose solutions, indicated on Fig. 2, where both the viscosity η and the refractive index n of the solution depend on the concentration of the additive. Since the refractive index of bulk PDMS is 1.403 [19], films on solutions with refractive indices near this value are inaccessible; for both substances considered here, this inaccessible range corresponded to bulk viscosities between about 3 and 20 times that of water (see barred region in Fig. 2).

In order to study the relaxation of domains in a monolayer, it is necessary to produce isolated domains of an appropriate size with respect to the resolution and field of view of the microscope, deform them, and then hope that the relaxation times fall within the limits set by the speed

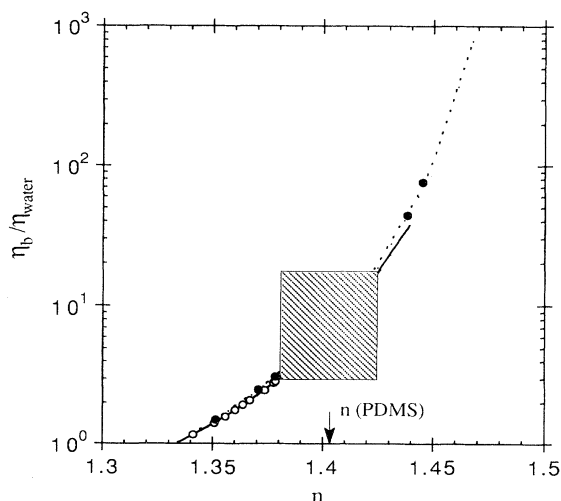


FIG. 2. Bulk viscosity n as a function of refractive index n for glycerol (dashed line) and glucose (solid line) solutions. Data are from Ref. [42]. The refractive index is nearly linear in glucose or glycerol concentration. Viscosities of the different glycerol (●) and glucose (○) solutions used as substrates are indicated. Solutions with index $n \approx 1.40 \pm 0.02$ (barred region; for both glycerol and glucose, $3 < \eta_b/\eta_{\text{water}} < 20$) provide insufficient contrast with the polymer layer.

of image taking and the time that the domain remains within the field of view, typically limited by convection within the liquid.

In a carefully protected PDMS monolayer, typical domain sizes are much larger than the field of view; in fact the evidence suggests that after deposition of the polymer in a spreading solvent and evaporation of that solvent, most of the polymer can be found in a single large domain centered with respect to the trough [8,20]. This is clearly inappropriate for the present study. It was, however, observed that holes opened up in the dense polymer layer if the protective cover was removed, closing again when it was replaced. These holes were used in a preliminary relaxation study [8], but are clearly not ideal for the purpose. The mechanism behind the hole formation is not understood, but it is almost certainly not a static equilibrium process; the effect of this on the relaxation processes is unclear. Further, these holes form mostly in the vicinity of an edge between domains and if isolated, as desirable for relaxation experiments, disappear within a few seconds. While domains whose relaxation was obviously impeded by several surrounding domains were avoided, virtually all domains studied bordered one other domain, with an unknown influence on the relaxation processes. Finally, the necessary absence of the cover allows airflow above the surface and increases movement within it, greatly complicating the measurement.

However, the area of any dense polymer domains, unlike that of any holes in such domains, was unaffected by the presence or absence of the cover [8,20], regardless of the relative position of such domains. Dense domains of size smaller than the field of view were never observed after deposition with a spreading solvent, but appeared after sudden temperature changes or if polymer was removed from the surface with a suction device. They also appeared in the traces of the (carefully cleaned) stainless steel needle used to provide the shear forces that deformed domains, if that needle first passed through a dense polymer film.

It is this effect that is used in this work to apply the polymer to the liquid surface: A multilayer film is formed on a clean water surface to the side of the apparatus, applying the polymer either in a hexane spreading solvent or as a pure droplet. (In the latter case the majority of the polymer must be suctioned off to reduce the polymer surface concentration to levels corresponding to a few monolayer thicknesses. Measured relaxation times were independent of this initial deposition method, demonstrating that solvent effects are unimportant with this secondary deposition method.) The needle is drawn through the multilayer film and then brought to the surface under the microscope. The size of the domains formed in this way can be partially controlled by the (multilayer) polymer surface concentration in the separate dish and by the speed at which the needle is drawn through the liquid surface under the microscope.

Surface tension measurements, used as a first control to any effect of the glycerol or glucose on the polymer monolayer, were made by the Wilhelmy method using a platinum open-frame probe, a fine horizontal wire (0.19 mm in diameter and 20 mm long) fixed in a fine wire

frame [21]; more usual probe shapes, the plate and the ring, yielded anomalies in measurements on the insoluble polymer layer [8,20]. The open frame probe gave results in agreement with other methods and literature data for the insoluble monolayer on water and in agreement with the plate method, within the ± 0.1 mN/m precision of that measurement, for standard soluble surfactant solutions [20]. Reproducibility with the open frame probe on a given surface is ± 0.02 mN/m and the overall accuracy is estimated at ± 0.2 mN/m. The polymer was applied to the surface in dilute hexane spreading solutions.

Experiments were performed at room temperature $22 \pm 1^\circ\text{C}$. The sample cell was a round trough, 70 mm in diameter, with a polished glass bottom and a Teflon rim. It was cleaned with a sulfochromic acid solution and occasionally an additional wash of alcoholic sodium hydroxide. The trough was protected by a glass cover. To limit convection in the Brewster angle microscopy experiments, the liquid level was limited to about 3 mm, the minimum depth before light scattered from the trough bottom began to interfere seriously with the image quality.

The polymer samples were of molecular weight $M_w = 10\,000$ ($M_w/M_n = 1.13$) and $100\,000$ ($M_w/M_n = 1.23$). Glycerol and glucose were analytical grade from Prolabo or Merck; solutions were left in contact with activated charcoal (Prolabo, analytical grade) for several hours and then filtered, in order to remove surfactant impurities. Without this treatment, the surface tension of the resulting solutions decreased slightly with time and impurities were evident in the microscopic images of the surface. The viscosity η_b/ρ of the solutions was measured with a capillary viscometer and remained unchanged over the course of the experiments. The hexane used in any spreading solutions was from Merck (analysis grade).

RESULTS AND DISCUSSION

Glycerol and glucose were added to the water substrate in order to increase its viscosity, to allow investigation of the influence of that viscosity on domain relaxation. The possibility that these additives may also change the character of the polymer layer should not be ignored. The behavior of fatty acids on glycerol has been found to be similar, but not identical, to that on pure water [22]. A first test is the comparison of the surface tension isotherms for the polymer on the various solutions. This is presented in Fig. 3 for a 20% glucose solution and for 20% and 80% glycerol solutions, corresponding to the range of solutions used in the relaxation experiments.

We can see that, within the experimental accuracy, there are no significant differences between the isotherms for surface pressures below about 5 mN/m: In all cases the surface pressure (the change in the surface tension in the presence of the polymer) remains unmeasurably low until concentrations above 0.6 mg/m, where the surface pressure suddenly increases. On all substrates, the same curve is followed as this pressure increases, but deviations occur as the surface pressure levels out to a plateau value when the polymer film begins to collapse out of the sim-

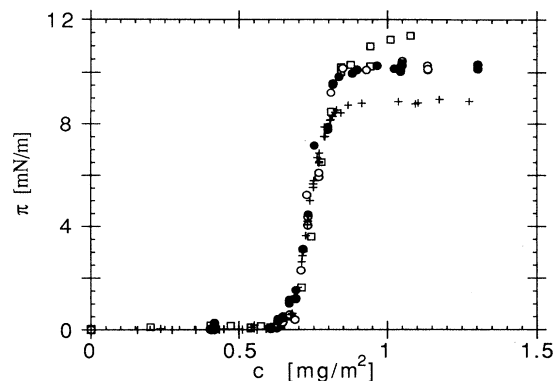


FIG. 3. Surface pressure isotherms, PDMS on pure water (+) and on glucose (20%, solid circles) and glycerol (open symbols: 20%, circles; 80%, squares) solutions.

ple monolayer state [8,23]. This plateau is higher on the 20% glycerol and glucose solutions; on the concentrated glycerol solution, the surface pressure continues to increase. This may indicate the presence of glycerol or glucose in the collapsed layer. Note that the plateau values on the glucose and 20% glycerol solutions are identical, suggesting that the effect of these two molecules on the state of the collapsed monolayer is similar.

The presence of glycerol or glucose in the solution clearly does influence the collapse process. All the work presented here is, however, in the very low polymer concentration zone (at $\pi \sim 0$ mN/m, with coexistence between dense and very dilute polymer domains); the additives have no discernible influence on the surface pressure even as the concentration is increased out of this zone. It has been shown [23] that this surface pressure increase is consistent with the power-law behavior of a two-dimensional polymer in a poor solvent. At higher pressures, again ~ 5 mN/m, deviations from the power-law behavior occur; the polymer certainly changes not just its local density but its configuration with respect to the surface, which here would seem to be affected by the additives to the water substrate. However, the good agreement in the power-law zone suggests that the nature of polymer layers of lesser density, and thus the polymer domains to be studied here, is affected little by the glucose or glycerol. The behavior of the domains could be more sensitive than the surface pressure to any influence of the additives, but any such effect should depend directly on the additive concentration, while the bulk viscosity is very nonlinear in that concentration (Fig. 2). Thus a study of the relaxation on substrate solutions with a wide range of different viscosities may allow one to test for the influence of glycerol or glucose on the nature of the polymer layer; the relaxation times are unlikely to have a simple dependence on substrate viscosity unless the viscosity itself is the major variable and other effects of the glycerol or glucose negligible.

Three examples of polymer domain relaxation are given in Fig. 4. The apparently simple relaxation of a monolayer domain toward a circular shape involves quite complicated hydrodynamics, with movement both in the

monolayer domain toward a circular shape involves quite complicated hydrodynamics, with movement both in the monolayer itself and in the substrate dragged along with that monolayer. Two limits offer some hope of an analytical solution. Small deformations are expected to follow an exponential relaxation law; this was demonstrated in the previous work [8] on the PDMS films to hold even to quite significant deformations. The opposite extreme, that of bola, or two heads and a thin connecting strip, has been recently treated by Benvegnu and McConnell [7]. As long as the heads are significantly wider than the connecting strip, the relaxation is observed to occur by simple shortening of the connecting strip, with little change in the size and shape of the heads [see Figs. 4(a) and 4(c)]. In this quasi-steady-state, a restoring force due to the nearly constant Laplace pressure difference across the domain must be balanced by a nearly constant viscous dissipation, or a nearly constant velocity. Most of what follows will be focused on the small deformation case, but results for bola relaxation will be discussed for comparison.

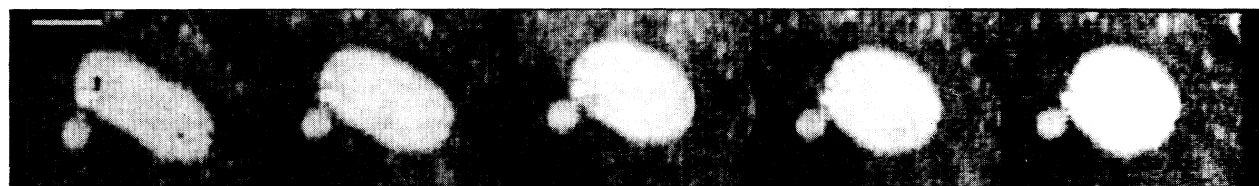
In the small deformation limit, it is useful to have some simple definition of that deformation. Since the relaxation is driven by a tendency to shorten the perimeter P of the domain, under the constraint of constant area A (as-

suming that the monolayer is essentially incompressible; this should be verified), the most natural definition is the reduced curve length $P/(4\pi A)^{1/2}$. The perimeter is, however, difficult to measure accurately: any imperfections in the image reflect strongly in the measurement. A much simpler definition for the deformation, $\Theta \equiv (L/W) - 1$, where L is the length and W the width of the domain, can be measured much more accurately, generally to 1% even with the very poor contrast available as the refractive index of the substrate approaches that of the polymer layer. Further, this measure of the distortion, unlike the reduced curve length, can readily be corrected for some of the sources of systematic error in the observed distortions.

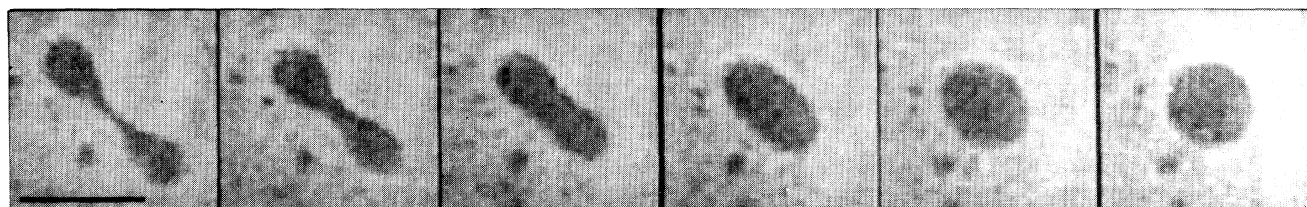
There are several sources for this error: (1) an optical distortion of 5–10% for objects of size $\sim 100 \mu\text{m}$, depending on the position of within the field of view; (2) movement during the imaging process, which is greatly reduced as the viscosity is increased—for the same minimum substrate depth, convection decreases markedly, and the response to any mechanical disturbance (such as that produced during the initial distortion of the domains) is minimized; and (3) the halo effect for images taken in a single, out-of-focus band [see Fig. 4(c)]. Domains typically appear elongated perpendicular to the



(a)



(b)



(c)

FIG. 4. Relaxation in a PDMS monolayer (a) hole in a layer on pure water, 3.5 sec/frame; (b) dense domain on 85% glycerol solution ($\eta_b/\eta_{\text{water}}=80$), 50 sec/frame; and (c) dense domain on glucose solution ($\eta_b/\eta_{\text{water}}=1.4$), 0.4 sec/frame. Bars in left frames represent $50 \mu\text{m}$.

in-focus line. Corrections for these effects combined may be made with respect to nearby objects (typically distorted by $\sim 10\%$ in a well-defined direction), but a residual $\sim 5\%$ uncertainty leads to an uncertainty $\sim 15\%$ in the deduced relaxation times, assuming that the relaxation can be followed over a range $1 \gtrsim \Theta \gtrsim 0.1$.

The measurement of the domain area is also influenced by these factors, leading to a typical 5% uncertainty on the domain size $R \equiv (A/\pi)^{1/2}$. The measured areas of dense domains were constant within this accuracy. This accuracy can be improved if the domain remains stationary in the center of the field of view. This has occurred, on very highly concentrated glycerol solutions [Fig. 4(b)]; the domain area was constant during the relaxation, within the 1% precision of the measurement, and over a period of more than 30 min. On the other hand, polymer holes tend to close, frequently decreasing in area by more than 10% over a few seconds.

The assumption of an incompressible dense polymer layer is thus experimentally reasonable. The elasticity, or inverse of the compressibility, can in fact be deduced as ~ 10 mN/m at 600 Hz, from the stationary value in the partial monolayer measured by the forced capillary wave method [24]. This is well within the incompressible range (see the Appendix).

Typical relaxation curves are given in Fig. 5. For deformation $\Theta \geq 2$, the end radius $r_{\text{bola}} = W/2$ remains approximately constant as the ends approach with nearly constant speed: Θ decreases linearly in time, $\theta = \theta_0 - Vt/r_{\text{bola}}$ [see Fig. 5(a)]. This is the "bola" relaxation previously studied by Benvegnu and McConnell [7]. For relatively small deformations ($\Theta \leq 1$), the relaxation appears to follow an exponential law $\Theta \sim e^{-t/T_c}$, where T_c is a characteristic relaxation time. This behavior can be clearly seen in a semilogarithmic scale [Fig. 5(b)]: note one atypical example in which the domain (filled circles), on a very viscous glycerol solution, happened to be very steady in the center of the field of view during the whole ($\Theta \leq 1$) relaxation process. This happenstance minimized experimental errors and provided a particularly good test for exponential relaxation, with a positive result.

The reduced relaxation times, that is, the characteristic relaxation time divided by the bulk viscosity relative to that of water, for moderate ($\Theta \leq 1$) deformations are presented in Fig. 6 as a function of average domain radius $R \equiv (A/\pi)^{1/2}$. A range of bulk viscosities is grouped under a single symbol for clarity. The scatter is considerably larger than expected from the uncertainty in the individual measurements, typically 15% on T_c and 5% on R . In fact, several factors extraneous to the line tension and viscosities may affect this relaxation. First, nearby domains certainly influence the relaxation. Figure 4(a) is in fact one example of this; you can see that the line on one edge of the domain visibly deforms as the domain relaxes. This influence is readily observable for distances up to approximately the domain size, as would be expected from hydrodynamic effects since the fluid, in the substrate and in any polymer layer, is in motion for distances of this order. In the presence of nearby stationary domains, relaxation times tend to be increased by a factor of 2 or 3 [25]. If, on the other hand, neighboring

domains are themselves in motion, the relaxation times may either increase or decrease depending on the relative placement and motion of the domains. Since the hydrodynamic effects extend to distances of the order of the domain size, reliable data for very large domains were extremely difficult to achieve; one requires that such domains, necessarily few and far between, decide to relax within the field of view of the microscope. The probability appears minimal. Relaxation times for domains with $R > 30 \mu\text{m}$ are thus sparse and should be treated with caution. Such measurements might be possible (for a different physical system) in fluorescence microscopy experiments, where electric fields have been used to manipulate, isolate, and hold stationary such domains [26,6]; no such probe can approach the laser beam in the Brewster

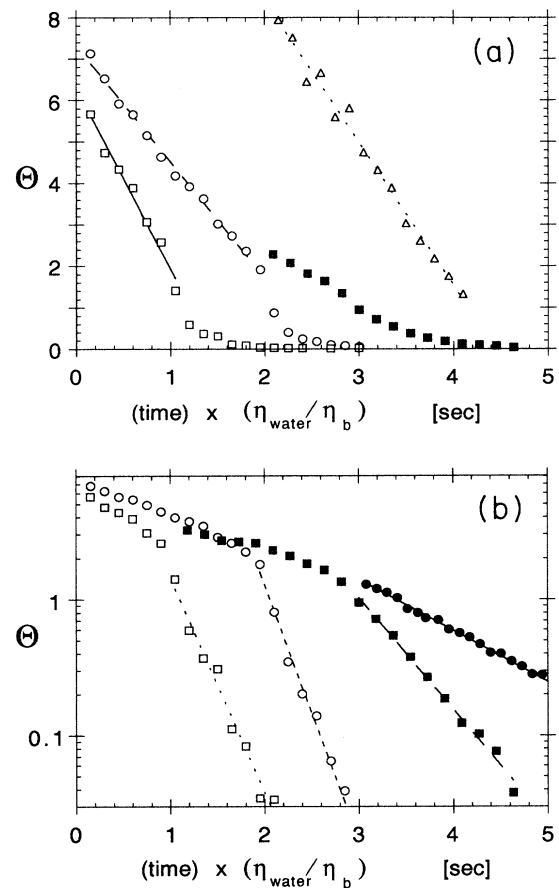


FIG. 5. Relaxation in a PDMS monolayer; deformation Θ (see the text) as a function of time t . (a) For $\Theta > 2$, the radius of the ends (r_{bola}) remains approximately constant and Θ decreases linearly with time $\Theta = \Theta_0 - Vt/r_{\text{bola}}$; (b) for $\Theta < 1$, the relaxation is exponential $\Theta = \Theta_0 e^{-t/T_c}$. Where possible, the same domain is shown in the two relaxation regimes: \square , $r_{\text{bola}} = 8 \mu\text{m}$, $R = (A/\pi)^{1/2} = 16 \mu\text{m}$, on water; \circ , $r_{\text{bola}} = 7 \mu\text{m}$, $R = 13 \mu\text{m}$, on water; ∇ , $r_{\text{bola}} = 9.5 \mu\text{m}$, on water; \blacksquare , $R = 28 \mu\text{m}$, on glucose, $\eta_b/\eta_{\text{water}} = 2.2$; \bullet , $R = 43 \mu\text{m}$, on glycerol, $\eta_b/\eta_{\text{water}} = 75$. (a) Solid line, $V/r_{\text{bola}} = 4.37$ sec; long-dashed line, $V/r_{\text{bola}} = 2.7$ sec; dotted line, $V/r_{\text{bola}} = 3.44$ sec. (b) Solid line, $T_c = 88$ sec; long-dashed line, $T_c = 1.9$ sec; short-dashed line, $T_c = 0.28$ sec; dotted line, $T_c = 0.31$ sec.

angle microscope without swamping the signal.

The relaxation times also change with contamination of the surface, as demonstrated by the appearance of significant quantities of three-dimensional particles or, under exceptional circumstances, surfactant domains much more brilliant than any observed in a clean layer. Relaxation times again typically increased by a factor of 2 or 3 in such cases.

While there is significant scatter, for the reasons discussed above, the data are seen to fall on a single curve, which is fit well by a power law with exponent 2. This is the value expected if it is the bulk viscosity that dominates the relaxation dynamics. In fact, one expects

$$T_c \propto \begin{cases} \frac{\eta_s R}{\lambda} & \text{if the surface viscosity dominates} \\ \frac{\eta_b R^2}{\lambda} & \text{if the bulk viscosity dominates.} \end{cases}$$

The dependence on R can be seen on purely dimensional grounds; a more detailed discussion is presented in the Appendix.

In order to explore any subtle dependence on the bulk viscosity, not necessarily evident within the experimental scatter of Fig. 6, Fig. 7 gives a reduced relaxation rate, scaled by $R^2 \eta_b$ and grouped by domain size interval: no significant viscosity dependence is observed in this quantity, implying that the relaxation rate is in fact proportional to the bulk viscosity. Both these facts are consistent with dissipation dominated by the bulk viscosity and inconsistent with that dominated by the surface viscosity, for which the relaxation times would be independent of the bulk viscosity and linear in the average domain radius. This is contrary to the tentative con-

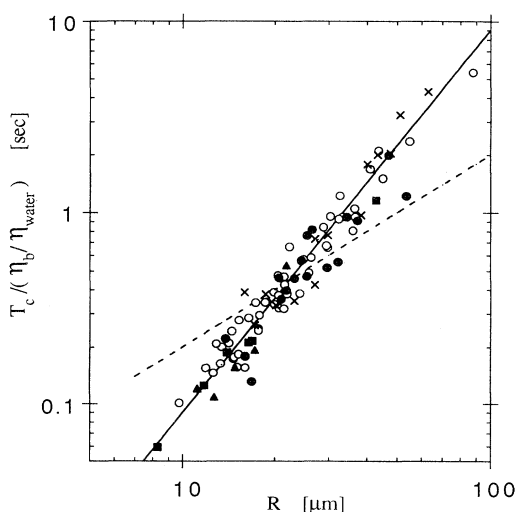


FIG. 6. Relative relation times as a function of domain size $R = (A/\pi)^{1/2}$, PDMS on water (\times), and solutions of glucose (open symbols, $1.2 < \eta_b/\eta_{\text{water}} < 3.2$) and glycerol (closed symbols; circles, $1.5 < \eta_b/\eta_{\text{water}} < 3.2$; triangles $\eta_b/\eta_{\text{water}} = 42$; squares, $\eta_b/\eta_{\text{water}} = 75$). Solid line, $T_c/(\eta_b/\eta_{\text{water}}) = 0.09 R^2 \text{ sec}/\mu\text{m}^2$; dashed line, $T_c/(\eta_b/\eta_{\text{water}}) = 0.002 R \text{ sec}/\mu\text{m}$.

clusions of Ref. [8], where the relaxation times were measured over a smaller range in relaxation times and at a single bulk viscosity and the necessity of extending the measurements under more favorable conditions, carried through in the present work, was acknowledged.

The fact that such a simple, consistent size and viscosity dependence is observed over a wide range of bulk viscosities and of size does suggest that the simple picture holds: that the characteristic of the domain that governs this relaxation is its line tension, uninfluenced by the presence of glucose or glycerol in the substrate, and furthermore that the effective viscosity observed in the relaxation is simply that of the bulk fluid. One can conclude that the viscosity near the surface on the micrometer scale remains similar to that of the bulk liquid.

Now that the source of the dissipation is well established, for moderate domain sizes $10 \mu\text{m} < R < 30 \mu\text{m}$, one would also like to establish the parameter driving the relaxation: the line tension. The quantity plotted in Fig. 7 is in fact proportional to the line tension on dimensional grounds alone. The prefactor has been determined, assuming that the monolayer viscosity is everywhere constant, by Stone and McConnell [27] (see the Appendix below): they find $T_c = 5\pi\eta_b R^2/16\lambda$, leading to an estimate $\lambda = (1.2 \pm 0.3) \times 10^{-12} \text{ N}$. In our case, any polymer layer at the exterior of the domain is very dilute; it is both much less viscous and much more compressible than the dense monolayer (see the Appendix for a discussion of the compressibility question in the hydrodynamical context). The expression of Stone and McConnell is no longer exact; with fewer constraints on the bulk fluid flow, the viscous effect may be slightly less, and the true surface tension somewhat lower, than that given here (see the Appendix).

A comparison with a complementary relaxation measurement, that of bola where the ends travel with essentially constant speed, may help establish this number. As long as the heads are significantly wider than the connecting strip, the relaxation is observed to occur by simple shortening of the connecting strip, with little change in the size and the shape of the heads. The energy gained in reducing the length, and thus energy, of the central strip is then balanced by the energy lost in dissipation; a steady state at constant velocity is expected. This is in fact observed [7], as can be seen in Fig. 5(a).

A first approximation in calculating the dissipation is to treat the two heads as circular and independent. This has been treated in the literature [7,28]. In the purely two-dimensional case, the treatment necessitates including the nonlinear terms in the Naviers-Stokes equation, exactly as for a cylinder in a three-dimensional fluid [29]. If the two-dimensional fluid sits on a substrate, the effect of this substrate viscosity dominates the nonlinear two-dimensional (2D) terms for physical systems; the bulk viscosity is thus expected to influence the relaxation whatever the relative bulk and surface viscosities; note that this consideration does not apply to such movement as the rotation of the domain [28] or the relaxation of a slightly deformed domain, which are solvable with the simple linear 2D Naviers-Stokes equation. In the other extreme, where the bulk viscosity dominates, the pres-

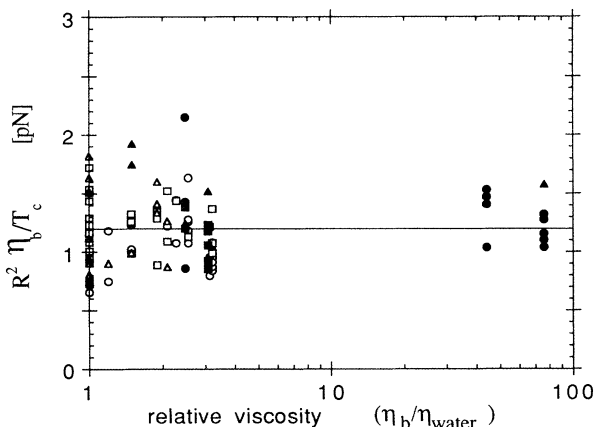


FIG. 7. Normalized relaxation rates as a function of bulk viscosity: open symbols, glucose; closed symbols, glycerol; all with $M_w = 100\,000$. Symbols at $\eta_b/\eta_{\text{water}} = 1$, pure water (open symbols, $M_w = 100\,000$; closed symbols, $M_w = 10\,000$). Divided into size ranges: circles, $r < 20\ \mu\text{m}$; squares, $20 < r < 30\ \mu\text{m}$; triangles, $r > 30\ \mu\text{m}$.

ence of an incompressible 2D fluid, of even very low viscosity, around the moving disk would increase the dissipation (by a factor of 1.5 as the surface viscosity decreases towards zero) since movement of the disk sets up movement in the 2D fluid, which influences the flow in the bulk above and beyond the direct motion of the disk.

The net result of these arguments is that one expects a single disk of radius R at the end of a string (where the second disk is not necessarily within the field of view) to travel with speed $V = \lambda/4\eta R$ if the disk is considered to sit in a 2D incompressible fluid or $V = 3\lambda/8\eta R$ if it is not.

Figure 8 gives the value of $4V\eta R$ in function of domain size. Considerable scatter is observed, but a line tension $\lambda = (1.1 \pm 0.3) \times 10^{-12}\ \text{N}$ is deduced, in excellent agreement with the small-deformation value given above. Note, however, that in both cases we are assuming that the regions surrounding the domain are incompressible with a finite viscosity. In the present case, any polymer film surrounding the dense domains is very dilute; it is not clear that it can be considered as hydrodynamically incompressible (see the Appendix below). The actual line tensions may be a factor of $\frac{2}{3}$ lower than this value. It might be interesting to compare the two cases of dense domains and holes in such domains, which might be expected to behave differently under these conditions. Unfortunately, isolated holes in the PDMS layer are not stable in time: holes close rapidly unless they are very close to other such holes [8,20]. It is thus difficult to obtain reliable data for the relaxation of these domains.

Note that in this analysis we have assumed that the line tension is a well-defined quantity, independent of domain shape and size, and in particular that long-range electrostatic effects, due to the average dipole moment perpendicular to the polymer layer, are negligible. In the size range studied ($R = 10\text{--}100\ \mu\text{m}$), the measured line tension is in fact independent of domain size and consistent between the two relaxation regimes, with very

different domain shapes. The expected electrostatic effects may be estimated, without ambiguity as to the dielectric constant of the interfacial region [8,20,30], from measurements of the surface potential difference between phases: λ_e , the contribution to the line energy due to electrostatic effects, is given by [6,7]

$$\lambda_e \sim \frac{(\Delta V)^2 \epsilon_0}{4\pi} \ln(r/h) = 1 \times 10^{-13}\ \text{N}$$

for domains with characteristic dimension r in the range $10\text{--}100\ \mu\text{m}$, where the measured potential difference is $0.12\ \text{V}$ [31] and the molecular parameter h is taken as $0.4\ \text{nm}$, the average distance between monomers in the dense phase. Note that this correction is an order of magnitude less than the measured line tension. It is thus expected to be negligible, as in fact observed.

CONCLUSIONS

Previous studies on the hydrodynamics in monolayers of small molecules have assumed that dissipation occurs dominantly in the substrate [7]. Flow patterns within the monolayer forced through a channel support this hypothesis [32]. Here it has been clearly and directly demonstrated that the viscous drag on movement within a monolayer of the polymer PDMS is also dominated by the bulk viscosity, at least in the domain size range $10\ \mu\text{m} < R < 30\ \mu\text{m}$. One would expect a crossover to domination by the surface viscosity for $\eta_s/\eta_b R > 1$. Attempts [33] to measure η_s have resulted only in an estimate of an upper limit: $\eta_s < 10^{-2}\ \text{mg}/\text{sec}$, which would correspond to $R = 10\ \mu\text{m}$ for the upper limit for crossover on a pure water substrate. Our data confirm this upper limit. It is difficult to imagine extending this limit by optical methods. However, PDMS is unusually flexible with an unusually low viscosity for a polymer, in surface and in bulk (where the glass temperature is -120°) [34]. Virtually any surface-active polymer would be expected to have a higher surface viscosity, and if the polymer also forms island domains similar to those in PDMS monolayers, as is expected for polymethylmethacrylate for example [33,35], it might be possible to observe such a crossover, with the bulk viscosity as an additional param-

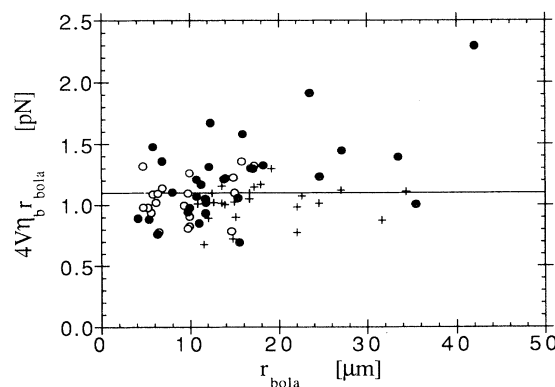


FIG. 8. Relaxation of bola (large deformation limit) on various aqueous substrates: normalized speed V vs end radius R . Substrates: glycerol (\bullet), glucose (\circ), and pure water ($+$).

eter. This could provide simultaneous estimates of both the line energy and the surface viscosity, both of which are difficult to obtain otherwise.

We find consistent line tension estimates from the two limits: low deformation and bola relaxation. Some questions remain, particularly when one phase is very dilute, and that phase of the monolayer can no longer be approximated as incompressible. It would be interesting to extend the calculation of Stone and McConnell [27] to this case. An analytical solution over the whole range of possible domain shape has been explored in the context of the mathematical analysis of the evolution of plane contours to a circular form yielding what are called curve-shortening equations [36]. To date, these solutions require assuming a drag force local to the boundary rather than the more realistic bulk and surface viscosities. Comparing relaxation of distorted domains in films near a shape instability limit, Seul [13] finds partial agreement with this analytic solution, but systematic deviations at large distortions. This implies a nonlocal, shape-dependent term, either to the surface tension, as would be expected as one approaches a point where the electrostatic forces compete with the local line tension to produce shape instabilities, also observed, or due to the nonlocal (to the boundary) nature of the viscous forces. In fact, the bola relaxation described above, a reasonable (and observed) physical solution to relaxation on a viscous substrate [37], does not follow the curve shortening equation. While this approach is extremely interesting, it appears not yet entirely applicable to the physical situation.

In spite of these ambiguities, an approximate, consistent line tension can be deduced from the data presented here: $\lambda = (1.1 \pm 0.3) \times 10^{-12}$ N; the actual value may be a factor of $\frac{2}{3}$ lower. In either case, this is low compared to the expected value $\lambda \sim 1 \times 10^{-11}$ N. In a simple bond-breaking model, the line tension would be related to an interaction distance δ by $\lambda \sim k_B T / \delta$. The line tension observed here implies that δ is approximately ten times the average monomer separation, ~ 0.4 nm. The origin of this low line tension remains unclear.

The contrast in surface concentration between phases and the relatively high monolayer elasticity do not suggest the approach of a critical point. On the other hand, something like a critical point does occur in function of molecular mass: no domain separation is observed for $M_w = 1250$. However, no difference in the line tension is seen at higher molecular weights, here $M_w = 10\,000$ and $100\,000$; these low line tensions are thus quite unlike those due to the classical influence of a nearby critical point. The behavior of the polymer layers at different molecular masses is being explored to clarify this point.

ACKNOWLEDGMENTS

E.K.M. would like to thank Pascal Silberzan, David Lubensky, and J. Adin Mann, Jr. for many fruitful discussions. The Laboratoire de Physique Statistique is URA 1306 du CNRS, associées aux Universités Paris VI and Paris VII.

APPENDIX: SMALL DISTORTION LIMIT FOR 2D DOMAIN RELAXATION

In order to describe the relaxation of domains in a two-dimensional film on a fluid substrate, one must consider the momentum balance in the fluid (given by the Naviers-Stokes equation), the force balance at the interface (given by a two-dimensional Naviers-Stokes equation with an additional term from the stress on the monolayer due to movement in the underlying fluid), and the normal and tangential force balance at the domain boundary. It is the normal, Laplace, force at this boundary that is expected to drive the domain relaxation. On a fluid such as water, the viscosity of the substrate alone is expected to be sufficient to place the system in the overdamped limit. Even ignoring all inertial terms and considering small distortions, the hydrodynamics are far from trivial.

In the noninertial limit and assuming that the velocity of the fluid and the surface are continuous, the linearized two-dimensional Naviers-Stokes equation is given by [38]

$$0 = -\nabla_s \pi + \eta_s \nabla_s^2 \mathbf{v}_s - \eta_b \left[\frac{\partial \mathbf{v}_s}{\partial z} + \nabla_s v_z \right]_{z=0}, \quad (\text{A1})$$

where the last term completes the tangential force balance at the interface, representing the stress on the surface due to flow in the underlying fluid. The subscripts s refer to the quantities in the plane of the surface, b refers to quantities in the bulk, π is the surface pressure, η refers to the viscosity, and z is defined as the direction normal to the plane, pointing out of the fluid.

As a first approximation, assume a two-dimensional incompressible fluid

$$0 = \nabla_s \cdot \mathbf{v}_s. \quad (\text{A2})$$

Within the bulk fluid, the usual Navier-Stokes equation will hold

$$0 = -\nabla P + \eta_b \nabla^2 \mathbf{v}, \quad (\text{A3})$$

where P is the bulk pressure and η_b the bulk viscosity. The bulk fluid will certainly be incompressible: $0 = \nabla \cdot \mathbf{v}$. We are searching for solutions for which $v_z = 0$; the incompressibility of the substrate may make this impossible, in the same way that longitudinal waves necessarily involve a vertical, capillary component at the asymmetric air-fluid interface [39].

At the domain boundary, the normal force balance is given by the Laplace law

$$\Delta \pi = \lambda / R_c, \quad (\text{A4})$$

where $\Delta \pi$ is the change in surface pressure across the boundary, λ is the line tension, and R_c is the local radius of curvature. Assume that the boundary is given in polar coordinates (ρ, ϕ) by

$$\rho = R_0(1 + \varepsilon \cos n \phi), \quad \varepsilon \ll 1, \quad (\text{A5})$$

that is, consider relaxation of a mode n of very small amplitude. Note that the relaxation studied above is the lowest relaxation mode $n = 2$ and that in the limit $\varepsilon \ll 1$, the definition of the deformation used in the main body of the article is given by $\Theta = 2\varepsilon$. The radius of curvature is

then given to first order in ε by

$$\begin{aligned} 1/R_c &= \frac{\left[\rho^2 + 2 \left[\frac{\partial \rho}{\partial \phi} \right]^2 - \rho \frac{\partial^2 \rho}{\partial \phi^2} \right]}{\left[r^2 + \left[\frac{\partial \rho}{\partial \phi} \right]^2 \right]^{3/2}} \\ &= \frac{1 + (n^2 - 1)\varepsilon \cos n\phi}{R_0}. \end{aligned} \quad (\text{A6})$$

The tangential force balance at the boundary depends on the viscoelasticity of the line. This is expected to be negligible in the absence of a line-active agent in the same way that the surface viscoelasticity of a pure liquid is usually assumed negligible. Assuming no line viscoelasticity,

$$\begin{aligned} 0 &= \eta_s^{\text{exterior}} \left[\frac{1}{\rho} \frac{\partial \mathbf{v}_\rho}{\partial \phi} + \rho \frac{\partial(\mathbf{v}_\phi/\rho)}{\partial \rho} \right]_{r=R_0(1+\varepsilon \cos n\phi)^+} \\ &- \eta_s^{\text{interior}} \left[\frac{1}{\rho} \frac{\partial \mathbf{v}_\rho}{\partial \phi} + \rho \frac{\partial(\mathbf{v}_\phi/\rho)}{\partial \rho} \right]_{r=R_0(1+\varepsilon \cos n\phi)^-}. \end{aligned} \quad (\text{A7a})$$

The opposite extreme would be to assume an infinite boundary elasticity, or

$$v_\phi|_{\rho=R_0(1+\varepsilon \cos n\phi)^+} = v_\phi|_{\rho=R_0(1+\varepsilon \cos n\phi)^-}. \quad (\text{A7b})$$

It is useful to use reduced coordinates for simplicity:

$$\begin{aligned} r^* &= r/R_0, \quad z^* = z/R_0, \quad t^* = \frac{\lambda}{\eta_b R_0^2} t, \\ \eta_s^{\text{interior}} &= \alpha \eta_b \quad \text{inside domain boundary,} \\ \eta_s^{\text{exterior}} &= \beta \eta_b \quad \text{outside domain boundary,} \\ \mathbf{v}^* &= \frac{\eta_b R_0}{\lambda} \mathbf{v}, \quad \pi^* = \frac{R_0}{\lambda} \pi, \quad P^* = \frac{R_0^2}{\lambda} P. \end{aligned} \quad (\text{A8})$$

The dependence of the relative importance of the bulk and surface viscosities on domain size R_0 is left explicit.

In reduced coordinates

$$\Delta \pi = 1 + (n^2 - 1)\varepsilon \cos n\phi \quad \text{at } r^* = 1 + \varepsilon \cos n\phi, \quad (\text{A4}')$$

$$0 = -\nabla_s \pi^* + \alpha R_0 \nabla_s^2 \mathbf{v}_s^* - \left[\frac{\partial \mathbf{v}_s^*}{\partial z^*} + \nabla_s v_z^* \right]_{z=0} \quad (\text{A1}')$$

(replace α by β outside boundary),

$$0 = -\nabla P^* + \nabla^2 \mathbf{v}^*. \quad (\text{A3}')$$

The form of the remaining equations remains unchanged.

For $v_z|_{z=0}=0$, [1] and [2] imply $\nabla^2 \pi = 0$ so that from [4-6]

$$\pi^* = \begin{cases} \pi_0^* + 1 + a\rho^{*n} \cos n\phi & \text{inside boundary} \\ \pi_0^* + b\rho^{*-n} \cos n\phi & \text{outside boundary,} \end{cases} \quad (\text{A9a})$$

$$\pi_0^* = \begin{cases} \pi_0^* + 1 + a\rho^{*n} \cos n\phi & \text{inside boundary} \\ \pi_0^* + b\rho^{*-n} \cos n\phi & \text{outside boundary,} \end{cases} \quad (\text{A9b})$$

where

$$a - b = (n^2 - 1)\varepsilon. \quad (\text{A9c})$$

The analytic resolution the resulting set of equations is not obvious. The limiting case for which $\alpha + \beta \gg R_0$ can be solved.

1. Limit $\eta_s \gg \eta_b R$

In this case, only the surface equations need be considered and standard methods lead to solutions for the velocity components:

$$v_\rho^* = \begin{cases} n \left[A + \frac{aR_0 \rho^2}{4\alpha(n+1)} \right] \rho^{n-1} \cos n\phi & \text{inside boundary} \\ n \left[B + \frac{bR_0 \rho^2}{4\beta(n-1)} \right] \rho^{-n-1} \cos n\phi & \text{outside boundary} \end{cases} \quad (\text{A10a})$$

and

$$v_\phi^* = \begin{cases} -n \left[A + \frac{aR_0 \rho^2}{4\alpha(n+1)} (1+2/n) \right] \rho^{n-1} \sin n\phi & \text{inside boundary} \\ n \left[B + \frac{bR_0 \rho^2}{4\beta(n-1)} (1-2/n) \right] \rho^{-n-1} \sin n\phi & \text{outside boundary} \end{cases} \quad (\text{A10b})$$

Since the velocity must be continuous across the domain boundary,

$$A + \frac{aR_0}{4\alpha(n+1)} = B + \frac{bR_0}{4\beta(n-1)}, \quad (\text{A11a})$$

$$A + \frac{aR_0}{4\alpha(n+1)} (1+2/n) = - \left[B + \frac{bR_0}{4\beta(n-1)} (1-2/n) \right]. \quad (\text{A11b})$$

In order to complete the description, one must consider the tangential force balance at the domain boundary given by (A7). Assuming null boundary viscoelasticity, (A7a) leads to

$$v_\rho^* = \begin{cases} -n \frac{\varepsilon R_0}{4(\alpha + \beta)} [n + 1 - (n - 1)\rho^2] \rho^{n-1} \cos n\phi & \text{inside boundary} \\ n \frac{\varepsilon R_0}{4(\alpha + \beta)} [n - 1 - (n + 1)\rho^2] \rho^{-n-1} \cos n\phi & \text{outside boundary} \end{cases} \quad (\text{A12})$$

Since $d\varepsilon/dt^* = v_\rho^*$ for $\rho = 1$ and $\phi = 0$, this leads directly to

$$\varepsilon = \varepsilon_0 e^{-t/T_c}$$

$$\text{with } T_c = 4(\eta_s^{\text{interior}} + \eta_s^{\text{exterior}})R_0/2n\lambda. \quad (\text{A13})$$

The relaxation observed in this article is dominantly of the lowest nontrivial order $n = 2$, since the shear force deformation was of that symmetry and higher-order deformations relax much more quickly. For $n = 2$, $T_c = (\eta_s^{\text{interior}} + \eta_s^{\text{exterior}})R_0/\lambda$. Note that this simple expression is symmetric: dense monolayer domains and holes in such domains will relax at the same rate.

2. Limit $\eta_s \ll \eta_b R$

In this case, movement in both the bulk and in the surface must be considered and it is difficult to solve the resulting set of equations analytically. A simple approximation to the movement in the bulk liquid has been used by Ahmad and Hansen [40] (and extended by Joos and Pintens [41]) to explore the spreading kinetics of liquids (or monolayers) on liquids, with surprising success. In this approximation, one assumes that at the surface

$$\frac{\partial \mathbf{v}_s^*}{\partial z^*} = \frac{\mathbf{v}_s^*}{\xi}, \quad (\text{A14})$$

where ξR_0 is the penetration depth of the movement into the liquid. In very shallow liquid, this would correspond to a velocity decreasing linearly into the liquid and the penetration depth is simply the depth h of the dish [40]. In the opposite extreme, the comparison is with longitudinal waves on a liquid surface [39], with an exponential decay into the liquid [41]. The experimental case treated here corresponds to $h \gg R_0$ and the penetration depth would be simply proportional to R_0 , as expressed in [14]. Equation (A1') can then be rewritten

$$0 = -\nabla_s \pi^* - \mathbf{v}_s^*/\xi. \quad (\text{A15})$$

If the surface viscosity is neglected, only the normal components of the continuity equations at the boundary are relevant and in this approximation Eq. (9), for the surface pressure π^* , gives v_ρ^* directly:

$$v_\rho^* = \begin{cases} -an\xi\rho^{*n-1} \cos n\phi & \text{inside boundary} \\ bn\xi\rho^{*-n-1} \cos n\phi & \text{outside boundary} \end{cases}, \quad (\text{A16})$$

where Eq. (A9c) holds. The result depends on whether one assumes (a) incompressible 2D fluids on both sides of boundary, where by continuity of the velocity across the

boundary, $a = -b = (n^2 - 1)\varepsilon/2$, yielding

$$T_c = \frac{2\eta_b R_0^2}{n(n+1)\xi\lambda} \left[= \frac{\eta_b R_0^2}{3\xi\lambda} \text{ for } n=2 \right], \quad (\text{A17a})$$

or (b) 2D fluid on one side only of the boundary, where, as expected to hold for our experiments, a (or $-b$) = $(n^2 - 1)\varepsilon/2$ and

$$T_c = \frac{\eta_b R_0^2}{n(n+1)\xi\lambda} \left[= \frac{\eta_b R_0^2}{6\xi\lambda} \text{ for } n=2 \right]. \quad (\text{A17b})$$

Estimating ξ depends on finding a solution to the motion in the bulk fluid.

The complete problem has been solved very recently by Stone and McConnell [27] in the approximation in which the entire monolayer is assumed to be incompressible with the same (finite) viscosity. They find

$$T_c = \frac{\eta_b R_0^2}{\lambda} \frac{(2n+1)(2n-1)\pi}{4n^2(n^2-1)}, \quad (\text{A18})$$

when the bulk viscosity dominates.

This does not correspond exactly to our case: here the monolayer is very dilute on one side of the boundary, where it is both much less viscous and much more compressible. The more critical hypothesis may be that of incompressibility. The condition for hydrodynamical incompressibility may be estimated simply: the characteristic variation of the density $\Delta\rho$ must be much less than the density ρ : $1 \gg \Delta\rho/\rho \approx \Delta\pi/\varepsilon$, where ε is the elasticity, or the inverse of the compressibility. But from the Laplace equation [Eq. (A4)], the pressure difference across a domain is given by the line tension and the variation in the line curvature: $\Delta\pi \sim \lambda\Delta(1/R_c) \lesssim \lambda/R$. A surface phase may thus be considered incompressible if $\varepsilon \gg \lambda/R \approx 10^{-4}$ mN/m, for the values $\lambda \sim 10^{-12}$ N and $R \sim 10$ μm typical for this experiment. The condensed phase has elasticity $\varepsilon \sim 10$ mN/m [24] and easily fulfills this criteria. The elasticity in the gaseous phase is difficult to estimate. It is certainly less than the elasticity of an ideal gas ε_I because of the attraction between polymer chains: $\varepsilon < \varepsilon_I = \rho RT/M_w \approx (\rho_{\text{gas}}/\rho_{\text{dense}})10^{-2}$ mN/m, for our system with $M_w = 10^5$ and the density of the condensed phase $\rho_{\text{dense}} \sim 0.6$ mg/m². Unfortunately, it is difficult to estimate the density of the dilute phase ρ_{gas} . The onset of phase coexistence cannot be estimated from surface pressure vs area data because the surface pressures are unmeasurably small in this whole domain. Ellipsometry [23] (Fig. 1) implies an upper limit $(\rho_{\text{gas}}/\rho_{\text{dense}}) < 10^{-1}$. Surfaces are

much too inhomogeneous for a reasonable estimate from either the onset of coexistence or the relative fractions of the gaseous and condensed phases in the microscopic measurements (where the field of view is $\sim 10^{-4}$ of the total surface), but they do suggest $(\rho_{\text{gas}}/\rho_{\text{dense}}) < 10^{-2}$. The compressibility of these gaseous films should probably not be neglected for motion in which the substrate viscosity provides the limiting force.

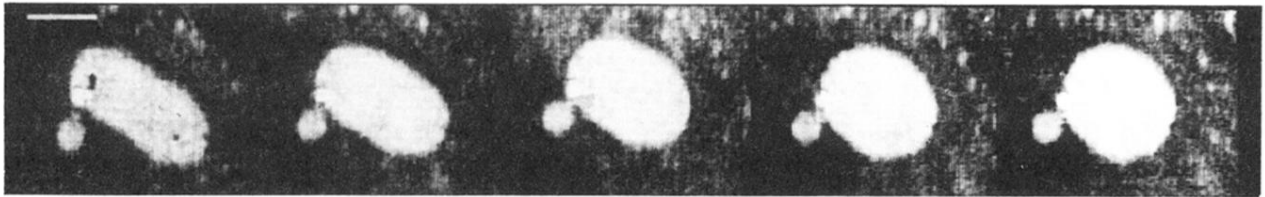
The error made by the approximation in which the whole monolayer is considered as incompressible with a single surface viscosity is, however, unlikely to be more than a factor of 2; for the opposite extreme of bola relaxation, the relaxation in the presence of a monolayer is a factor of $\frac{3}{2}$ faster than if the monolayer is entirely ignored. A similar factor is plausible here.

- [1] N. K. Adam, *The Physics and Chemistry of Surfaces* (Oxford University Press, London, 1941); A. W. Adamson, *Physical Chemistry of Surfaces*, 5th ed. (Wiley, New York, 1990).
- [2] M. Lösche, E. Sackmann, and H. Möhwald, *Ber. Bunsenges. Phys. Chem.* **87**, 848 (1983); H. M. McConnell, L. K. Tann, and R. M. Weiss, *Proc. Natl. Acad. Sci. USA* **81**, 3249 (1984); R. M. Weiss and H. M. McConnell, *Nature* **310**, 3249 (1984); H. E. Gaub, V. T. Moy, and H. M. McConnell, *J. Phys. Chem.* **90**, 1721 (1985).
- [3] S. Hénon and J. Meunier, *Rev. Sci. Instrum.* **62**, 936 (1991); D. Hönig and D. Möbius, *J. Phys. Chem.* **95**, 4590 (1991).
- [4] C. Knobler, in *Advances in Chemical Physics*, edited by I. Prigogine and S. A. Rice (Wiley, New York, 1990), Vol. 77, p. 397.
- [5] F. Gallet and P. Müller, *Phys. Rev. Lett.* **67**, 1106 (1991).
- [6] H. M. McConnell, P. A. Rice, and D. J. Benvegnu, *J. Phys. Chem.* **94**, 8965 (1990); J. F. Klingler and H. M. McConnell, *ibid.* **97**, 2962 (1993); D. J. Benvegnu and H. M. McConnell, *ibid.* **97**, 6686 (1993).
- [7] D. J. Benvegnu and H. M. McConnell, *J. Phys. Chem.* **96**, 6820 (1992).
- [8] E. K. Mann, S. Hénon, D. Langevin, and J. Meunier, *J. Phys.*, (France) **II 2**, 1693 (1992).
- [9] *Light Scattering by Liquid Surfaces and Complementary Measures*, edited by D. Langevin (Dekker, New York, 1992).
- [10] M. Seul and M. J. Sammon, *Phys. Rev. Lett.* **64**, 1903 (1990); M. Seul, *Physica A* **168**, 198 (1990); M. Seul and M. J. Sammon, *Rev. Sci. Instrum.* **62**, 784 (1991).
- [11] For the most favorable case, where bulk viscosity dominates, critical damping is for $\eta_b/(\rho_b\lambda)^{1/2} \sim 1$, or $\lambda \sim 10^{-9}$ N, much larger than the $\lambda \sim 10^{-11}$ N expected for monolayer systems: Overdamping is expected in these systems whenever material movement within the monolayer, and thus within the bulk, is involved. Overdamping is expected for lines between domains of different densities, but not necessarily for lines between domains of different molecular orientation for example. [S. Rivière, S. Hénon, and J. Meunier, *Phys. Rev. E* **49**, 1375 (1994).]
- [12] M. Kahlweit and W. Ostner, *Chem. Phys. Lett.* **18**, 589 (1973).
- [13] M. Seul, *J. Phys. Chem.* **97**, 2941 (1993).
- [14] W. Fox, P. W. Taylor, and W. A. Zisman, *Ind. Eng. Chem.* **39**, 1401 (1947); M. J. Newing, *Trans. Faraday Soc.* **46**, 755 (1950); W. Noll, H. Steinbach, and C. Sucker, *Ber. Bunsenges. Phys. Chem.* **67**, 407 (1963).
- [15] L. T. Lee, E. K. Mann, D. Langevin, and B. Farnoux, *Langmuir* **7**, 3076 (1991).
- [16] S. Hénon and J. Meunier, *J. Chem. Phys.* **94**, 9148 (1993).
- [17] Note that the absolute value of the ellipticity, and thus the reflectivity, is actually less for the dense polymer phase than for pure water; dense polymer domains appear dark.
- [18] P. Drude, *Ann. Phys. Chem. (Leipzig)* **43**, 91 (1891).
- [19] Rhône Poulenc documentation on silicon oil, series 47.
- [20] E. K. Mann, Doctoral thesis, Université de Paris VI, 1992 (unpublished).
- [21] N. K. Adam, *The Physics and Chemistry of Surfaces* (Ref. [1]), p. 383; A. Lenard, *Ann. Phys. (Leipzig)*, **74**, 381 (1924).
- [22] A. Barraud, J. Leloup, and P. Lesieur, *Thin Solid Films* **133**, 113 (1985).
- [23] E. K. Mann, L. T. Lee, S. Hénon, D. Langevin, and J. Meunier, *Macromolecules* **26**, 7037 (1993).
- [24] E. K. Mann and D. Langevin, *Langmuir* **7**, 1112 (1991).
- [25] In fact, the previously reported data [8], in which neighboring domains were necessarily present as discussed above, showed relaxation times about twice those reported here.
- [26] A. Miller, C. A. Helm, and H. Möhwald, *J. Phys. (Paris)* **48**, 693 (1987); T. K. Vanderlick and H. Möhwald, *J. Phys. Chem.* **94**, 886 (1990).
- [27] H. A. Stone and H. M. McConnell, *Proc. R. Soc. London Ser. A* **448**, 97 (1995).
- [28] B. D. Hughes, B. A. Pailthorpe, and L. R. White, *J. Fluid Mech.* **110**, 349 (1981).
- [29] In fact, the vorticity induced by the motion of a disk in a two-dimensional fluid is such that the Brownian motion model for viscosity does not converge, leading to doubts as to the definition of a two-dimensional viscosity, independent of time scale.
- [30] S. Rivière, S. Hénon, J. Meunier, G. Albrecht, M. M. Boissonnade, and A. Baszkin (unpublished).
- [31] M. D. Bennett and W. A. Zisman, *Macromolecules* **4**, 47 (1971).
- [32] D. K. Schwartz, C. M. Knobler, and R. Bruinsma, *Phys. Rev. Lett.* **73**, 2841 (1994).
- [33] N. L. Jarvis, *J. Phys. Chem.* **70**, 3027 (1966); G. Hard and R. D. Neumann, *J. Colloid Interface Sci.* **120**, 15 (1987).
- [34] W. Noll, *Chemistry and Technology of Silicones* (Academic, London, 1968); *Silicon-Based Polymer Science*, edited by J. M. Zeigler and F. W. G. Fearon (American Chemical Society, Washington, DC, 1990).
- [35] R. Vilanove, D. Poupinet, and F. Rondelez, *Macromolecules* **21**, 2880 (1988); M. Kawaguchi, M. Tohyama, Y. Mutoh, and A. Takahashi, *Langmuir* **4**, 407 (1988); B. B. Sauer, H. Yu, and G. Zograf, *Macromolecules* **22**, 2332 (1989); M. Kawaguchi, B. B. Sauer, and G. Yu, *ibid.* **22**, 1735 (1989).
- [36] S. A. Langer, R. E. Goldstein, and D. P. Jackson, *Phys. Rev. A* **46**, 4894 (1992).
- [37] The stability of the connecting band might be influenced by electrostatic effects.

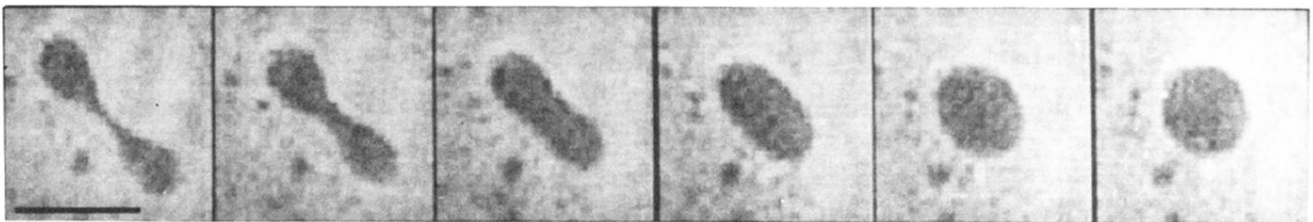
- [38] F. C. Goodrich, Proc. R. Soc. London Ser. A **374**, 341 (1981).
- [39] E. H. Lucassan-Reynders and J. Lucassen, Adv. Colloid Interface Sci. **2**, 347 (1969).
- [40] J. Ahmad and R. S. Hansen, J. Colloid Interface Sci. **38**, 601 (1972).
- [41] P. Joos and J. Pintens, J. Colloid Interface Sci. **60**, 507 (1977).
- [42] *CRC Handbook of Physics and Chemistry*, 54th ed. (CRC, Boca Raton, FL, 1973).



(a)



(b)



(c)

FIG. 4. Relaxation in a PDMS monolayer (a) hole in a layer on pure water, 3.5 sec/frame; (b) dense domain on 85% glycerol solution ($\eta_b/\eta_{\text{water}}=80$), 50 sec/frame; and (c) dense domain on glucose solution ($\eta_b/\eta_{\text{water}}=1.4$), 0.4 sec/frame. Bars in left frames represent $50\ \mu\text{m}$.